Determination of second-order nonlinear coefficients in semiconductors using pseudospin equations for three-level systems

D. C. Hutchings and J. M. Arnold
Department of Electronics and Electrical Engineering, University of Glasgow, Glasgow G12 8QQ, United Kingdom
(Received 19 March 1997)

A pseudospin formalism is developed for analyzing the dynamics of a three-level system analogous to the Maxwell-Bloch equations in the two-level case. These are used in the nonresonant regime to obtain the complete and general form of the second-order optical susceptibility. All the nonzero second-order tensor elements for second-harmonic generation are calculated for bulk GaAs and asymmetric GaAs/$Al_xGa_{1-x}As$ quantum wells. It is demonstrated that a partial cancellation of terms occurs which limits the values obtained in the asymmetric quantum wells. It is also demonstrated by example that the band structure can also strongly influence the values obtained. While small values are obtained for the examples given here, it is reasoned that large second-order susceptibilities should be obtainable with short-period asymmetric superlattices. [S0163-1829(97)08131-9]

I. INTRODUCTION

There is intense current interest in semiconductor waveguides for second-order nonlinear optical applications. These include second-harmonic generation, difference frequency generation, parametric generation and amplification, optical rectification, the electro-optic effect,[1,2] and all-optical switching and solitons using the cascade process.[3] Not only do semiconductors have larger second-order coefficients than commonly used second-order nonlinear crystals [GaAs has a second-order susceptibility $\chi^{(2)}_{xyz}$ of around 300 pmV^{-1} in the near ir (Ref. 4)], but the mature fabrication technology lends itself to device integration, particularly with semiconductor diode lasers. However, the principal deficit is that cubic semiconductors lack birefringence and hence phase matching is not trivial.

There are currently three principal techniques under investigation to solve this phase-matching problem. First, birefringence can be introduced structurally (e.g., waveguide).[5,6] However, the degree of birefringence possible in this case is limited and it is likely to be difficult to compensate for dispersion in the near-resonant frequency regime where large nonlinear coefficients are obtainable. Second, quasi-phase-matching by domain reversal is possible using patterned substrate growth[7,8] (an extension of the stack of plates technique[9,10]). This method shows promise although scattering problems at domain interfaces still have to be fully resolved. Third, second-order nonlinearities can be induced by introducing an asymmetry into the structure.[11,12] In this case a promising quasi-phase-matching technique is to periodically destroy this asymmetry by quantum well disordering.[13,14]

There have been a number of theory papers discussing the magnitude of second-order nonlinear coefficients for second-harmonic generation in asymmetric semiconductor heterostructures.[15–25] It is interesting to note that predictions as large as several hundred pmV^{-1} have been predicted for the second-order susceptibility in the near ir and yet corresponding experimental measurements are of the order of 10 pmV^{-1}.[26–28] All of these theoretical papers apparently base their determination of the second-order coefficient on a density matrix formalism using an $\mathbf{E}\cdot\mathbf{r}$ dipole perturbation. The calculation is usually truncated so that only the most resonant term(s) are retained. A commonly quoted form for the second-order susceptibility has the difference between two terms containing dipole matrix elements $\mathbf{r}_{ab}$.[15–19,23,24] This form cannot be justified, as a rigorous derivation of the second-order susceptibility using an $\mathbf{E}\cdot\mathbf{r}$ dipole perturbation (for example, using the density matrix) provides an expression where all terms (whether resonant or nonresonant) have the same sign.[29] Furthermore, in semiconductors electrons are, in general, delocalized and momentum is a better quantum number than position. Therefore interband optical matrix elements are usually formulated in terms of momentum matrix elements. This is often accounted for with the substitution $e\mathbf{r}_{vc}\rightarrow -ie\mathbf{p}_{vc}/(m_0\omega)$. Clearly this substitution is not correct since the matrix elements contain no information about the optical field and a Hermitian operator is replaced by a non-Hermitian one. The correct form of substitution in this case is $e\mathbf{r}_{vc}\rightarrow -ie\mathbf{p}_{vc}/(m_0\omega_{vc})$.

Since momentum matrix elements are required for semiconductors, the approach we take here is to use an $\mathbf{A}\cdot\mathbf{p}$ dipole perturbation from the initial stages. Both forms of perturbation are equivalent although in principle a summation over all terms and energy levels is required to duplicate results from both approaches. A density-matrix approach to the derivation of nonlinear susceptibilities with an $\mathbf{A}\cdot\mathbf{p}$ perturbation is developed in Refs. 29 and 30. However, in the final expression for the susceptibility the relative signs of the various terms are not immediately obvious. One further deficiency of the standard density-matrix expression for the nonlinear susceptibility is that it is derived for one occupied and two vacant levels (although in principle the density-matrix approach could be reapplied with arbitrary population levels). For the near-ir operation, the contributing intersubband transition can occur between two valence subbands (initially occupied) in addition to between two electron subbands (initially vacant). A complete analysis would allow both possibilities to be addressed.

 © 1997 The American Physical Society

TABLE I. The generators of the SU(3) group (Refs. 32 and 33).

$$\lambda_1=\begin{pmatrix}0&1&0\\1&0&0\\0&0&0\end{pmatrix} \quad \lambda_2=\begin{pmatrix}0&0&0\\0&0&1\\0&1&0\end{pmatrix} \quad \lambda_3=\begin{pmatrix}0&0&1\\0&0&0\\1&0&0\end{pmatrix}$$

$$\lambda_4=\begin{pmatrix}0&i&0\\-i&0&0\\0&0&0\end{pmatrix} \quad \lambda_5=\begin{pmatrix}0&0&0\\0&0&i\\0&-i&0\end{pmatrix} \quad \lambda_6=\begin{pmatrix}0&0&i\\0&0&0\\-i&0&0\end{pmatrix}$$

$$\lambda_7=\begin{pmatrix}-1&0&0\\0&1&0\\0&0&0\end{pmatrix} \quad \lambda_8=\frac{1}{\sqrt{3}}\begin{pmatrix}-1&0&0\\0&-1&0\\0&0&2\end{pmatrix}$$

In this paper, pseudospin dynamical equations are derived to describe the dynamics of a three-level system (equivalent to the Maxwell-Bloch equations for a two-level system). These can be applied to a number of resonant nonlinear optical processes, for example, excited-state absorption, two-photon absorption, and electromagnetically induced transparency. Here the nonresonant regime will be taken and expressions are derived for the second-order susceptibility for both single and double occupancy of the levels in question. These are used to determine the second-order susceptibility for two example asymmetric quantum well structures. The consequences of the magnitude of these coefficients are discussed with an indication given on how useful coefficients can be obtained.

II. PSEUDOSPIN FORMALISM FOR THREE-LEVEL SYSTEM

The dynamical evolution of an N-level system can be expressed in terms of its $N\times N$ density matrix. Rather than consider each element of the density matrix individually, instead the density matrix and Hamiltonian will be expressed in terms of the N^2-1 matrices, λ_i which have SU(N) symmetry. In particular, for a three-level system, we will use as a basis the set of SU(3) generators in Table I.[31–33] The commutator relations between these matrices will be required;

$$[\lambda_i,\lambda_j]=\lambda_i\lambda_j-\lambda_j\lambda_i=\sum_k 2if_{ijk}\lambda_k, \tag{1}$$

where the nonzero structure factors f_{ijk} are permutations of those listed in Table II.

The time evolution of the expectation value of an operator is given by

$$\frac{d\langle\lambda_i\rangle}{dt}=-\frac{i}{\hbar}\langle[\lambda_i,H]\rangle. \tag{2}$$

The time-dependent Hamiltonian includes $\mathbf{A}(t)\cdot\mathbf{p}$ coupling between all three levels,

TABLE II. The value of the structure constant f_{ijk} in the commutator relations given by Eq. (1) between the SU(3) pseudospin matrices in Table I.

ijk	147	135	126	432	465	736	752	368	258
f_{ijk}	1	$-\frac{1}{2}$	$-\frac{1}{2}$	$-\frac{1}{2}$	$-\frac{1}{2}$	$\frac{1}{2}$	$\frac{1}{2}$	$\frac{\sqrt{3}}{2}$	$\frac{\sqrt{3}}{2}$

$$H(t)=\begin{pmatrix}\epsilon_a & \frac{e}{m_0}\mathbf{A}(t)\cdot\mathbf{p}_{ab} & \frac{e}{m_0}\mathbf{A}(t)\cdot\mathbf{p}_{ac}\\ \frac{e}{m_0}\mathbf{A}(t)\cdot\mathbf{p}^*_{ab} & \epsilon_b & \frac{e}{m_0}\mathbf{A}(t)\cdot\mathbf{p}_{bc}\\ \frac{e}{m_0}\mathbf{A}(t)\cdot\mathbf{p}^*_{ac} & \frac{e}{m_0}\mathbf{A}(t)\cdot\mathbf{p}^*_{bc} & \epsilon_c\end{pmatrix},$$

$$=\frac{\epsilon_a+\epsilon_b+\epsilon_c}{3}I+\frac{\epsilon_b-\epsilon_a}{2}\lambda_7+\frac{2\epsilon_c-\epsilon_b-\epsilon_a}{2\sqrt{3}}\lambda_8$$
$$+\frac{e}{m_0}\mathrm{Re}[\mathbf{A}(t)\cdot\mathbf{p}_{ab}]\lambda_1+\frac{e}{m_0}\mathrm{Re}[\mathbf{A}(t)\cdot\mathbf{p}_{bc}]\lambda_2$$
$$+\frac{e}{m_0}\mathrm{Re}[\mathbf{A}(t)\cdot\mathbf{p}_{ac}]\lambda_3+\frac{e}{m_0}\mathrm{Im}[\mathbf{A}(t)\cdot\mathbf{p}_{ab}]\lambda_4$$
$$+\frac{e}{m_0}\mathrm{Im}[\mathbf{A}(t)\cdot\mathbf{p}_{bc}]\lambda_5+\frac{e}{m_0}\mathrm{Im}[\mathbf{A}(t)\cdot\mathbf{p}_{ac}]\lambda_6, \tag{3}$$

where $\mathbf{p}_{ab}=\langle b|-i\hbar\nabla|a\rangle$ and ϵ_a, ϵ_b, and ϵ_c and the energies of the levels in the absence of the time-dependent coupling. Strictly speaking, the Hamiltonian in Eq. (3) should also contain a term proportional to the square of the vector potential $(eA)^2/(2m_0)$, but this is proportional to the identity matrix I, commutes with all the generator matrices, and therefore does not contribute to the dynamical equations. Solving Eq. (2) provides the equations of motion for the three-level system where we have substituted the real quantities $s_i=\langle\lambda_i\rangle$,

$$\frac{d}{dt}(s_1+is_4)=i\Omega_{ab}(s_1+is_4)-2i\frac{e}{m_0\hbar}\mathbf{A}\cdot\mathbf{p}_{ab}s_7$$
$$+i\frac{e}{m_0\hbar}\mathbf{A}\cdot\mathbf{p}^*_{bc}(s_3+is_6)$$
$$-i\frac{e}{m_0\hbar}\mathbf{A}\cdot\mathbf{p}_{ac}(s_2-is_5),$$

$$\frac{d}{dt}(s_2+is_5)=i\Omega_{bc}(s_2+is_5)-i\frac{e}{m_0\hbar}\mathbf{A}\cdot\mathbf{p}^*_{ab}(s_3+is_6)$$
$$+i\frac{e}{m_0\hbar}\mathbf{A}\cdot\mathbf{p}_{bc}(s_7-\sqrt{3}s_8)$$
$$+i\frac{e}{m_0\hbar}\mathbf{A}\cdot\mathbf{p}_{ac}(s_1-is_4),$$

$$\frac{d}{dt}(s_3+is_6)=i\Omega_{ac}(s_3+is_6)-i\frac{e}{m_0\hbar}\mathbf{A}\cdot\mathbf{p}_{ab}(s_2+is_5)$$
$$+i\frac{e}{m_0\hbar}\mathbf{A}\cdot\mathbf{p}_{bc}(s_1+is_4)$$
$$-i\frac{e}{m_0\hbar}\mathbf{A}\cdot\mathbf{p}_{ac}(s_7+\sqrt{3}s_8),$$

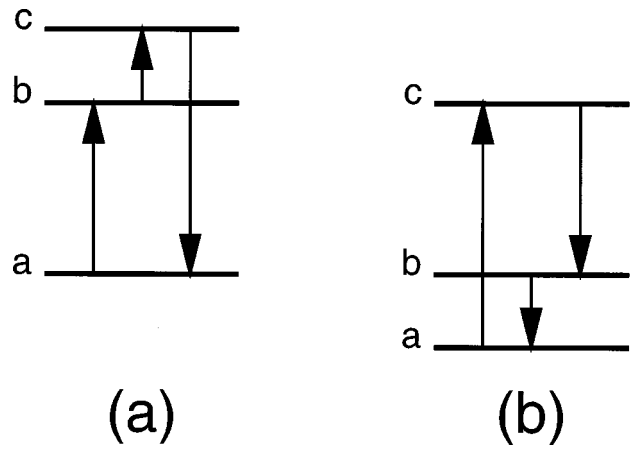

FIG. 1. Virtual transition schemes contributing to second-order optical nonlinearities. (a) initially has one filled state and two empty (e.g., multiple conduction states) and (b) initially has two filled states (e.g., multiple valence states). Note the time ordering in (b) leads to an exchange of electrons.

$$\frac{d}{dt}\,s_7 = -2\frac{e}{m_0\hbar}\,\mathrm{Im}[\mathbf{A}\cdot\mathbf{p}_{ab}(s_1 - is_4)] + \frac{e}{m_0\hbar}\,\mathrm{Im}[\mathbf{A}\cdot\mathbf{p}_{bc} \times (s_2 - is_5)] - \frac{e}{m_0\hbar}\,\mathrm{Im}[\mathbf{A}\cdot\mathbf{p}_{ac}(s_3 - is_6)],$$

$$\frac{d}{dt}\,s_8 = -\frac{\sqrt{3}e}{m_0\hbar}\,\mathrm{Im}[\mathbf{A}\cdot\mathbf{p}_{bc}(s_2 - is_5)] - \frac{\sqrt{3}e}{m_0\hbar}\,\mathrm{Im}[\mathbf{A}\cdot\mathbf{p}_{ac}(s_3 - is_6)]. \tag{4}$$

The energy differences have been written as $\hbar\Omega_{ab} = \epsilon_b - \epsilon_a$,etc.

The system of differential equations (4) can be regarded as the evolution of a real eight-dimensional pseudospin vector $\mathbf{S} = (s_1, s_2, s_3, s_4, s_5, s_6, s_7, s_8)^T$,

$$\frac{d\mathbf{S}}{dt} = \mathcal{M}\mathbf{S}. \tag{5}$$

A similar system has been employed to study the dynamics of a three-level atomic system with the following modifications:[33] (1) $\mathbf{E}\cdot\mathbf{r}$ dipole coupling is used, (2) coupling between the levels a and c is absent, and (3) near-resonant excitation is studied so the rotating-wave approximation is implemented and phenomenological damping terms are included. Here the purpose is to study the nonresonant excitation so Eq. (4) is left in its time-dependent form (so resonant and antiresonant terms will both be present) and it is not necessary to explicitly include damping. However, if required, dephasing can be included in Eq. (4) with the substitution $\Omega_{ij} \to \Omega_{ij} + i\gamma$.

The optical coupling will be taken to be the combination of two monochromatic waves at frequencies ω_1 and ω_2,

$$\begin{aligned}\mathbf{A}(t) &= -\int_{-\infty}^{t} \mathbf{E}(t')dt' \\ &= -\frac{i}{2\omega_1}\,[\mathbf{E}_1 e^{-i\omega_1 t} - \mathbf{E}_1^* e^{i\omega_1 t}] \\ &\quad -\frac{i}{2\omega_2}\,[\mathbf{E}_2 e^{-i\omega_2 t} - \mathbf{E}_2^* e^{i\omega_2 t}].\end{aligned} \tag{6}$$

Eventually contributions at the sum frequency $\omega_1 + \omega_2$ will be examined. Inserting in Eq. (4) and transforming to the frequency domain (making use of the Fourier shift theorem) provides

$$\begin{aligned}i\frac{m_0\hbar}{e}\,(\omega + \Omega_{ab})S_1(\omega) &= \left[\frac{\mathbf{E}_1 s_7(\omega - \omega_1) - \mathbf{E}_1^* s_7(\omega + \omega_1)}{\omega_1} + \frac{\mathbf{E}_2 s_7(\omega - \omega_2) - \mathbf{E}_2^* s_7(\omega + \omega_2)}{\omega_2}\right]\cdot\mathbf{p}_{ab} \\ &\quad -\left[\frac{\mathbf{E}_1 S_3(\omega - \omega_1) - \mathbf{E}_1^* S_3(\omega + \omega_1)}{2\omega_1} + \frac{\mathbf{E}_2 S_3(\omega - \omega_2) - \mathbf{E}_2^* S_3(\omega + \omega_2)}{2\omega_2}\right]\cdot\mathbf{p}_{bc}^* \\ &\quad +\left[\frac{\mathbf{E}_1 S_2^*(-\omega + \omega_1) - \mathbf{E}_1^* S_2^*(-\omega - \omega_1)}{2\omega_1} + \frac{\mathbf{E}_2 S_2^*(-\omega + \omega_2) - \mathbf{E}_2^* S_2^*(-\omega - \omega_2)}{2\omega_2}\right]\cdot\mathbf{p}_{ac},\end{aligned} \tag{7}$$

$$\begin{aligned}i\frac{m_0\hbar}{e}\,(\omega + \Omega_{bc})S_2(\omega) &= \left[\frac{\mathbf{E}_1 S_3(\omega - \omega_1) - \mathbf{E}_1^* S_3(\omega + \omega_1)}{2\omega_1} + \frac{\mathbf{E}_2 S_3(\omega - \omega_2) - \mathbf{E}_2^* S_3(\omega + \omega_2)}{2\omega_2}\right]\cdot\mathbf{p}_{ab}^* \\ &\quad -\left[\frac{\mathbf{E}_1 s_-(\omega - \omega_1) - \mathbf{E}_1^* s_-(\omega + \omega_1)}{2\omega_1} + \frac{\mathbf{E}_2 s_-(\omega - \omega_2) - \mathbf{E}_2^* s_-(\omega + \omega_2)}{2\omega_2}\right]\cdot\mathbf{p}_{bc} \\ &\quad -\left[\frac{\mathbf{E}_1 S_1^*(-\omega + \omega_1) - \mathbf{E}_1^* S_1^*(-\omega - \omega_1)}{2\omega_1} + \frac{\mathbf{E}_2 S_1^*(-\omega + \omega_2) - \mathbf{E}_2^* S_1^*(-\omega - \omega_2)}{2\omega_2}\right]\cdot\mathbf{p}_{ac},\end{aligned} \tag{8}$$

$$i\frac{m_0\hbar}{e}(\omega+\Omega_{ac})S_3(\omega)=\left[\frac{\mathbf{E}_1S_2(\omega-\omega_1)-\mathbf{E}_1^*S_2(\omega+\omega_1)}{2\omega_1}+\frac{\mathbf{E}_2S_2(\omega-\omega_2)-\mathbf{E}_2^*S_2(\omega+\omega_2)}{2\omega_2}\right]\cdot\mathbf{p}_{ab}$$
$$-\left[\frac{\mathbf{E}_1S_1(\omega-\omega_1)-\mathbf{E}_1^*S_1(\omega+\omega_1)}{2\omega_1}+\frac{\mathbf{E}_2S_1(\omega-\omega_2)-\mathbf{E}_2^*S_1(\omega+\omega_2)}{2\omega_2}\right]\cdot\mathbf{p}_{bc}$$
$$+\left[\frac{\mathbf{E}_1s_+(\omega-\omega_1)-\mathbf{E}_1^*s_+(\omega+\omega_1)}{2\omega_1}+\frac{\mathbf{E}_2s_+(\omega-\omega_2)-\mathbf{E}_2^*s_+(\omega+\omega_2)}{2\omega_2}\right]\cdot\mathbf{p}_{ac}, \tag{9}$$

where we define $S_1=s_1+is_4$, $S_2=s_2+is_5$, $S_3=s_3+is_6$, $s_-=s_7-\sqrt{3}s_8$, and $s_+=s_7+\sqrt{3}s_8$. Equations for $s_7(\omega)$ and $s_8(\omega)$ can also be derived by Fourier transform of $s_7(t)$ and $s_8(t)$ in Eq. (4) but the details of these are not necessary for nonresonant second-order nonlinearities.

From the pseudospin vector solution we can obtain the expectation value of the momentum,

$$\langle\mathbf{p}(\omega)\rangle=\frac{1}{2}\,[S_1(\omega)\mathbf{p}_{ab}^*+S_1^*(-\omega)\mathbf{p}_{ab}+S_2(\omega)\mathbf{p}_{bc}^*+S_2^*(-\omega)\mathbf{p}_{bc}+S_3(\omega)\mathbf{p}_{ac}^*+S_3^*(-\omega)\mathbf{p}_{ac}]. \tag{10}$$

Subsequently we can obtain the current and hence the polarization,

$$\mathbf{P}(\omega)=-i\,\frac{e}{m_0\omega}\sum\langle\mathbf{p}(\omega)+e\mathbf{A}(\omega)\rangle, \tag{11}$$

where the summation will be performed over combinations of three levels (e.g., for a solid this would involve the density of states).

The method of solution is a perturbative expansion as follows. First we obtain the pseudospin vector in the absence of optical coupling. For the coherence terms s_1-s_6, dephasing ensures that these tend to zero in the absence of the field. The population terms depend only on the initial occupation levels, $s_7(t)=N_b-N_a$ and $s_8(t)=(2N_c-N_b-N_a)/\sqrt{3}$. These initial values are substituted in Eqs. (7)–(9) to obtain the pseudospin vector to first order in the field amplitude. Then these first-order values are substituted again in Eqs. (7)–(9) to obtain the pseudospin vector to second order in the field amplitude. This process could be repeated to the required order. The second-order optical susceptibility is obtained by substitution of the second-order pseudospin vector into Eq. (11).

A. One occupied state

If state a is initially filled ($N_a=1$) and states b and c are empty ($N_b=N_c=0$) then the only non-zero expectation values of the pseudospin vector to order zero are $s_7^{(0)}(t)=-1$ and $s_8^{(0)}(t)=-1/\sqrt{3}$. Hence $s_7^{(0)}(\omega)=-\delta(\omega)$ and $s_8^{(0)}(\omega)=-\delta(\omega)/\sqrt{3}$. Inserting these in Eqs. (7)–(9) gives to the first order in the pseudospin vector

$$i\frac{m_0\hbar}{e}(\omega+\Omega_{ab})S_1^{(1)}(\omega)=-\left[\frac{\mathbf{E}_1\delta(\omega-\omega_1)-\mathbf{E}_1^*\delta(\omega+\omega_1)}{\omega_1}+\frac{\mathbf{E}_2\delta(\omega-\omega_2)-\mathbf{E}_2^*\delta(\omega+\omega_2)}{\omega_2}\right]\cdot\mathbf{p}_{ab},$$
$$i\frac{m_0\hbar}{e}(\omega+\Omega_{ac})S_3^{(1)}(\omega)=-\left[\frac{\mathbf{E}_1\delta(\omega-\omega_1)-\mathbf{E}_1^*\delta(\omega+\omega_1)}{\omega_1}+\frac{\mathbf{E}_2\delta(\omega-\omega_2)-\mathbf{E}_2^*\delta(\omega+\omega_2)}{\omega_2}\right]\cdot\mathbf{p}_{ac}, \tag{12}$$

and $S_2^{(1)}=s_7^{(1)}=s_8^{(1)}=0$.

Inserting Eq. (12) into Eq. (11) gives the usual form for the contribution at frequency ω_1 from the pair of states (a,b) to the first-order polarization,[29]

$$\mathbf{P}^{(1)}(\omega)\big|_{\omega_1}=\frac{e^2}{2m_0^2\hbar\omega_1^2}\sum\left[\frac{\mathbf{E}_1\cdot\mathbf{p}_{ab}\mathbf{p}_{ab}^*}{\Omega_{ab}+\omega_1}+\frac{\mathbf{E}_1\cdot\mathbf{p}_{ab}^*\mathbf{p}_{ab}}{\Omega_{ab}-\omega_1}\right]\delta(\omega-\omega_1). \tag{13}$$

The pseudospin vector to second-order is obtained by resubstituting Eq. (12) into Eqs. (7)–(9). For simplicity we only retain terms which contribute at frequencies $\pm(\omega_1+\omega_2)$,

$$S_1^{(2)}(\omega)\big|_{\pm(\omega_1+\omega_2)}=-\frac{e^2}{2m_0^2\hbar^2}\frac{1}{\omega_1\omega_2(\Omega_{ab}+\omega)}\left\{\left[\frac{(\mathbf{E}_1\cdot\mathbf{p}_{bc}^*)(\mathbf{E}_2\cdot\mathbf{p}_{ac})}{\Omega_{ac}+\omega-\omega_1}+\frac{(\mathbf{E}_1\cdot\mathbf{p}_{ac})(\mathbf{E}_2\cdot\mathbf{p}_{bc}^*)}{\Omega_{ac}+\omega-\omega_2}\right]\delta(\omega-\omega_1-\omega_2)\right.$$
$$\left.+\left[\frac{(\mathbf{E}_1^*\cdot\mathbf{p}_{bc}^*)(\mathbf{E}_2^*\cdot\mathbf{p}_{ac})}{\Omega_{ac}+\omega+\omega_1}+\frac{(\mathbf{E}_1^*\cdot\mathbf{p}_{ac})(\mathbf{E}_2^*\cdot\mathbf{p}_{bc}^*)}{\Omega_{ac}+\omega+\omega_2}\right]\delta(\omega+\omega_1+\omega_2)\right\}, \tag{14}$$

$$S_2^{(2)}(\omega)|_{\pm(\omega_1+\omega_2)} = -\frac{e^2}{2m_0^2\hbar^2}\frac{1}{\omega_1\omega_2(\Omega_{bc}+\omega)}\left\{\left[\frac{(\mathbf{E}_1\cdot\mathbf{p}_{ac})(\mathbf{E}_2\cdot\mathbf{p}_{ab}^*)}{\Omega_{ab}-\omega+\omega_1}+\frac{(\mathbf{E}_1\cdot\mathbf{p}_{ab}^*)(\mathbf{E}_2\cdot\mathbf{p}_{ac})}{\Omega_{ab}-\omega+\omega_2}-\frac{(\mathbf{E}_1\cdot\mathbf{p}_{ab}^*)(\mathbf{E}_2\cdot\mathbf{p}_{ac})}{\Omega_{ac}+\omega-\omega_1}\right.\right.$$
$$\left.-\frac{(\mathbf{E}_1\cdot\mathbf{p}_{ac})(\mathbf{E}_2\cdot\mathbf{p}_{ab}^*)}{\Omega_{ac}+\omega-\omega_2}\right]\delta(\omega-\omega_1-\omega_2)+\left[\frac{(\mathbf{E}_1^*\cdot\mathbf{p}_{ac})(\mathbf{E}_2^*\cdot\mathbf{p}_{ab}^*)}{\Omega_{ab}-\omega-\omega_1}+\frac{(\mathbf{E}_1^*\cdot\mathbf{p}_{ab}^*)(\mathbf{E}_2^*\cdot\mathbf{p}_{ac})}{\Omega_{ab}-\omega-\omega_2}-\frac{(\mathbf{E}_1^*\cdot\mathbf{p}_{ab}^*)(\mathbf{E}_2^*\cdot\mathbf{p}_{ac})}{\Omega_{ac}+\omega+\omega_1}\right.$$
$$\left.\left.-\frac{(\mathbf{E}_1^*\cdot\mathbf{p}_{ac})(\mathbf{E}_2^*\cdot\mathbf{p}_{ab}^*)}{\Omega_{ac}+\omega+\omega_2}\right]\delta(\omega+\omega_1+\omega_2)\right\}, \tag{15}$$

$$S_3^{(2)}(\omega)|_{\pm(\omega_1+\omega_2)} = -\frac{e^2}{2m_0^2\hbar^2}\frac{1}{\omega_1\omega_2(\Omega_{ac}+\omega)}\left\{\left[\frac{(\mathbf{E}_1\cdot\mathbf{p}_{bc})(\mathbf{E}_2\cdot\mathbf{p}_{ab})}{\Omega_{ab}+\omega-\omega_1}+\frac{(\mathbf{E}_1\cdot\mathbf{p}_{ab})(\mathbf{E}_2\cdot\mathbf{p}_{bc})}{\Omega_{ab}+\omega-\omega_2}\right]\delta(\omega-\omega_1-\omega_2)\right.$$
$$\left.+\left[\frac{(\mathbf{E}_1^*\cdot\mathbf{p}_{bc})(\mathbf{E}_2^*\cdot\mathbf{p}_{ab})}{\Omega_{ab}+\omega+\omega_1}+\frac{(\mathbf{E}_1^*\cdot\mathbf{p}_{ab})(\mathbf{E}_2^*\cdot\mathbf{p}_{bc})}{\Omega_{ab}+\omega+\omega_2}\right]\delta(\omega+\omega_1+\omega_2)\right\}. \tag{16}$$

Inserting the second-order pseudospin vector into Eq. (11) gives the second-order polarization at the sum frequency $\omega_1+\omega_2$,

$$\mathbf{P}^{(2)}(\omega)|_{\omega_1+\omega_2} = \frac{ie^3}{4m_0^3\hbar^2}\frac{\delta(\omega-\omega_1-\omega_2)}{\omega_1\omega_2(\omega_1+\omega_2)}\sum\left[\frac{\mathbf{p}_{ab}^*(\mathbf{E}_1\cdot\mathbf{p}_{bc}^*)(\mathbf{E}_2\cdot\mathbf{p}_{ac})}{(\Omega_{ab}+\omega_1+\omega_2)(\Omega_{ac}+\omega_2)}+\frac{\mathbf{p}_{ab}^*(\mathbf{E}_2\cdot\mathbf{p}_{bc}^*)(\mathbf{E}_1\cdot\mathbf{p}_{ac})}{(\Omega_{ab}+\omega_1+\omega_2)(\Omega_{ac}+\omega_1)}\right.$$
$$+\frac{\mathbf{p}_{ab}(\mathbf{E}_1\cdot\mathbf{p}_{bc})(\mathbf{E}_2\cdot\mathbf{p}_{ac}^*)}{(\Omega_{ab}-\omega_1-\omega_2)(\Omega_{ac}-\omega_2)}+\frac{\mathbf{p}_{ab}(\mathbf{E}_2\cdot\mathbf{p}_{bc})(\mathbf{E}_1\cdot\mathbf{p}_{ac}^*)}{(\Omega_{ab}-\omega_1-\omega_2)(\Omega_{ac}-\omega_1)}+\frac{\mathbf{p}_{bc}^*(\mathbf{E}_1\cdot\mathbf{p}_{ac})(\mathbf{E}_2\cdot\mathbf{p}_{ab}^*)}{(\Omega_{ab}-\omega_2)(\Omega_{ac}+\omega_1)}$$
$$+\frac{\mathbf{p}_{bc}^*(\mathbf{E}_2\cdot\mathbf{p}_{ac})(\mathbf{E}_1\cdot\mathbf{p}_{ab}^*)}{(\Omega_{ab}-\omega_1)(\Omega_{ac}+\omega_2)}+\frac{\mathbf{p}_{bc}(\mathbf{E}_1\cdot\mathbf{p}_{ac}^*)(\mathbf{E}_2\cdot\mathbf{p}_{ab})}{(\Omega_{ab}+\omega_2)(\Omega_{ac}-\omega_1)}+\frac{\mathbf{p}_{bc}(\mathbf{E}_2\cdot\mathbf{p}_{ac}^*)(\mathbf{E}_1\cdot\mathbf{p}_{ab})}{(\Omega_{ab}+\omega_1)(\Omega_{ac}-\omega_2)}+\frac{\mathbf{p}_{ac}^*(\mathbf{E}_1\cdot\mathbf{p}_{ab})(\mathbf{E}_2\cdot\mathbf{p}_{bc})}{(\Omega_{ab}+\omega_1)(\Omega_{ac}+\omega_1+\omega_2)}$$
$$\left.+\frac{\mathbf{p}_{ac}^*(\mathbf{E}_2\cdot\mathbf{p}_{ab})(\mathbf{E}_1\cdot\mathbf{p}_{bc})}{(\Omega_{ab}+\omega_2)(\Omega_{ac}+\omega_1+\omega_2)}+\frac{\mathbf{p}_{ac}(\mathbf{E}_1\cdot\mathbf{p}_{ab}^*)(\mathbf{E}_2\cdot\mathbf{p}_{bc}^*)}{(\Omega_{ab}-\omega_1)(\Omega_{ac}-\omega_1-\omega_2)}+\frac{\mathbf{p}_{ac}(\mathbf{E}_2\cdot\mathbf{p}_{ab}^*)(\mathbf{E}_1\cdot\mathbf{p}_{bc}^*)}{(\Omega_{ab}-\omega_2)(\Omega_{ac}-\omega_1-\omega_2)}\right]. \tag{17}$$

The sequence of three momentum matrix elements can be thought of as a closed loop of three virtual transitions as shown in Fig. 1(a). Equation (17) follows the standard form for the second-order polarization determined using density-matrix theory for an $\mathbf{A}\cdot\mathbf{p}$ perturbation. However, it is commonly written in the form that the sum over possible levels and permutations still has to be performed.[29,30] Here the complete form is presented for the term involving the three levels a, b, and c, which in terms of virtual transitions includes both $a\rightarrow b\rightarrow c\rightarrow a$ and $a\rightarrow c\rightarrow b\rightarrow a$. Now the product of the three momentum matrix elements round the closed loop of virtual transitions must be imaginary. This must be the case for the polarization $\mathbf{P}^{(2)}$ to be in phase with the driving electric field and ensure the second-order susceptibility is pure real for nonresonant excitation (note the factor of i in the prefactor).

Taking linearly polarized light we have, for example,

$$\mathbf{p}_{ab}^*(\hat{\mathbf{e}}_1\cdot\mathbf{p}_{bc}^*)(\hat{\mathbf{e}}_2\cdot\mathbf{p}_{ac}) = -\mathbf{p}_{ab}(\hat{\mathbf{e}}_1\cdot\mathbf{p}_{bc})(\hat{\mathbf{e}}_2\cdot\mathbf{p}_{ac}^*), \tag{18}$$

where $\hat{\mathbf{e}}_1$ and $\hat{\mathbf{e}}_2$ are the (real) unit polarization vectors parallel to $\mathbf{E}_1$ and $\mathbf{E}_2$, respectively. Therefore there is a partial cancellation of terms between the virtual transition schemes $a\rightarrow b\rightarrow c\rightarrow a$ and $a\rightarrow c\rightarrow b\rightarrow a$. A similar analysis based on an $\mathbf{E}\cdot\mathbf{r}$ perturbation leads to the result that the product of the dipole matrix elements is pure real and this partial cancellation is not obtained.

From Eq. (17) the second-order nonlinear susceptibility can be written for linearly polarized light,

$$\chi_{ijk}^{(2)}(\omega_1,\omega_2) = \frac{ie^3}{m_0^3\hbar^2\epsilon_0}\frac{1}{\omega_1\omega_2(\omega_1+\omega_2)}\sum\left\{\frac{p_{ab}^i p_{bc}^j p_{ac}^{k*}[\Omega_{ab}\omega_2+\Omega_{ac}(\omega_1+\omega_2)]}{(\Omega_{ab}-\omega_1-\omega_2)(\Omega_{ab}+\omega_1+\omega_2)(\Omega_{ac}-\omega_2)(\Omega_{ac}+\omega_2)}\right.$$
$$+\frac{p_{ab}^i p_{bc}^k p_{ac}^{j*}[\Omega_{ab}\omega_1+\Omega_{ac}(\omega_1+\omega_2)]}{(\Omega_{ab}-\omega_1-\omega_2)(\Omega_{ab}+\omega_1+\omega_2)(\Omega_{ac}-\omega_1)(\Omega_{ac}+\omega_1)}+\frac{p_{ab}^k p_{bc}^i p_{ac}^{j*}[\Omega_{ab}\omega_1-\Omega_{ac}\omega_2]}{(\Omega_{ab}-\omega_2)(\Omega_{ab}+\omega_2)(\Omega_{ac}-\omega_1)(\Omega_{ac}+\omega_1)}$$
$$+\frac{p_{ab}^j p_{bc}^i p_{ac}^{k*}[\Omega_{ab}\omega_2-\Omega_{ac}\omega_1]}{(\Omega_{ab}-\omega_1)(\Omega_{ab}+\omega_1)(\Omega_{ac}-\omega_2)(\Omega_{ac}+\omega_2)}-\frac{p_{ab}^j p_{bc}^k p_{ac}^{i*}[\Omega_{ab}(\omega_1+\omega_2)+\Omega_{ac}\omega_1]}{(\Omega_{ab}-\omega_1)(\Omega_{ab}+\omega_1)(\Omega_{ac}-\omega_1-\omega_2)(\Omega_{ac}+\omega_1+\omega_2)}$$
$$\left.-\frac{p_{ab}^k p_{bc}^j p_{ac}^{i*}[\Omega_{ab}(\omega_1+\omega_2)+\Omega_{ac}\omega_2]}{(\Omega_{ab}-\omega_2)(\Omega_{ab}+\omega_2)(\Omega_{ac}-\omega_1-\omega_2)(\Omega_{ac}+\omega_1+\omega_2)}\right\}, \tag{19}$$

where $p_{ab}^j=\hat{\mathbf{e}}_j\cdot\mathbf{p}_{ab}$, etc.

For the case of second-harmonic generation $\omega_2=\omega_1=\omega$ and Eq. (19) can be somewhat simplified,

$$\chi^{(2)}_{ijk}(\omega,\omega)=\frac{ie^3}{2m_0^3\hbar^2\epsilon_0\omega^2}\left\{\frac{p^i_{ab}(p^j_{bc}p^{k*}_{ac}+p^k_{bc}p^{j*}_{ac})(\Omega_{ab}+2\Omega_{ac})}{(\Omega_{ab}-2\omega)(\Omega_{ab}+2\omega)(\Omega_{ac}-\omega)(\Omega_{ac}+\omega)}-\frac{p^i_{bc}(p^j_{ab}p^{k*}_{ac}+p^k_{ab}p^{j*}_{ac})(\Omega_{ac}-\Omega_{ab})}{(\Omega_{ab}-\omega)(\Omega_{ab}+\omega)(\Omega_{ac}-\omega)(\Omega_{ac}+\omega)}\right.$$
$$\left.-\frac{p^{i*}_{ac}(p^j_{ab}p^k_{bc}+p^k_{ab}p^j_{bc})(2\Omega_{ab}+\Omega_{ac})}{(\Omega_{ab}-\omega)(\Omega_{ab}+\omega)(\Omega_{ac}-2\omega)(\Omega_{ac}+2\omega)}\right\}. \tag{20}$$

Equation (20) contains three terms. The second of these is proportional to the separation of the two upper levels Ω_{bc}. The combination of the first and third terms may also be proportional to Ω_{bc} in the lowest order. For example, the on-diagonal tensor elements (e.g., zzz) contain the same momentum matrix factor. The remaining frequency terms transform into the negative of each other by interchanging $\Omega_{ab}\leftrightarrow\Omega_{ac}$. Hence this combination of two terms is proportional to $\Omega_{ac}-\Omega_{ab}=\Omega_{bc}$. It is therefore anticipated that the overall contribution from the three levels may vanish as $\Omega_{bc}/\Omega_{ab}\rightarrow 0$.

B. Two occupied states

The pseudospin matrix formalism described above can be extended to describe the contribution to the nonlinear optical coefficients from a set of states where more than one is initially occupied as shown in Fig. 1(b). In semiconductors the obvious application is to include terms associated with multiple valence bands. To obtain the three level contribution to the second-order susceptibility, an analysis similar to that of Sec. II A is followed, but starting instead from the initial values $N_a=N_b=1$, $N_c=0$ and hence, $s^{(0)}_7(\omega)=0$ and $s^{(0)}_8(\omega)=-2\delta(\omega)/\sqrt{3}$. In this case the only non-zero first order pseudospin vector components are $S^{(1)}_2$ and $S^{(1)}_3$, which corresponds to the fact that only $a\rightarrow c$ and $b\rightarrow c$ optical transitions are initially allowed by the Pauli exclusion principle.

Taking the results for $S^{(1)}_2$ and $S^{(1)}_3$, the second-order terms $S^{(2)}_1$, $S^{(2)}_2$, and $S^{(2)}_3$ can be generated. Thus a second-order polarization is found from which the second-order susceptibility is obtained,

$$\chi^{(2)}_{ijk}(\omega_1,\omega_2)=\frac{-ie^3}{m_0^3\hbar^2\epsilon_0}\frac{1}{\omega_1\omega_2(\omega_1+\omega_2)}\sum\left\{\frac{p^i_{ac}p^{j*}_{ab}p^{k*}_{bc}[\Omega_{ac}\omega_2+\Omega_{bc}(\omega_1+\omega_2)]}{(\Omega_{ac}-\omega_1-\omega_2)(\Omega_{ac}+\omega_1+\omega_2)(\Omega_{bc}-\omega_2)(\Omega_{bc}+\omega_2)}\right.$$
$$+\frac{p^i_{ac}p^{k*}_{ab}p^{j*}_{bc}[\Omega_{ac}\omega_1+\Omega_{bc}(\omega_1+\omega_2)]}{(\Omega_{ac}-\omega_1-\omega_2)(\Omega_{ac}+\omega_1+\omega_2)(\Omega_{bc}-\omega_1)(\Omega_{bc}+\omega_1)}+\frac{p^k_{ac}p^{i*}_{ab}p^{j*}_{bc}[\Omega_{ac}\omega_1-\Omega_{bc}\omega_2]}{(\Omega_{ac}-\omega_2)(\Omega_{ac}+\omega_2)(\Omega_{bc}-\omega_1)(\Omega_{bc}+\omega_1)}$$
$$+\frac{p^j_{ac}p^{i*}_{ab}p^{k*}_{bc}[\Omega_{ac}\omega_2-\Omega_{bc}\omega_1]}{(\Omega_{ac}-\omega_1)(\Omega_{ac}+\omega_1)(\Omega_{bc}-\omega_2)(\Omega_{bc}+\omega_2)}-\frac{p^j_{ac}p^{k*}_{ab}p^{i*}_{bc}[\Omega_{ac}(\omega_1+\omega_2)+\Omega_{bc}\omega_1]}{(\Omega_{ac}-\omega_1)(\Omega_{ac}+\omega_1)(\Omega_{bc}-\omega_1-\omega_2)(\Omega_{bc}+\omega_1+\omega_2)}$$
$$\left.-\frac{p^k_{ac}p^{j*}_{ab}p^{i*}_{bc}[\Omega_{ac}(\omega_1+\omega_2)+\Omega_{bc}\omega_2]}{(\Omega_{ac}-\omega_2)(\Omega_{ac}+\omega_2)(\Omega_{bc}-\omega_1-\omega_2)(\Omega_{bc}+\omega_1+\omega_2)}\right\}. \tag{21}$$

This form can be generated from the previous result in Eq. (19) using the following rules. The time ordering of the transitions changes from $a\rightarrow b$, $b\rightarrow c$, $c\rightarrow a$ to $a\rightarrow c$, $b\rightarrow a$, $c\rightarrow b$ [Fig. 1(b)]. Hence the momentum matrix elements transform, $\mathbf{p}_{ab}\rightarrow\mathbf{p}_{ac}$, $\mathbf{p}_{bc}\rightarrow\mathbf{p}^*_{ab}$, and $\mathbf{p}^*_{ac}\rightarrow\mathbf{p}^*_{bc}$. The frequency denominators denote the energy mismatch after each virtual transition (divided by Planck's constant) and hence the transformations $\Omega_{ab}\rightarrow\Omega_{ac}$ and $\Omega_{ac}\rightarrow\Omega_{bc}$ are performed. Finally, this set of virtual transitions leads to an exchange of electrons in states a and b so an additional Fermi factor of (-1) must also be included. This set of transformation rules has previously been applied to determining the third-order effects of two-photon absorption[34] and nonlinear refraction[35,36] in semiconductors.

III. BULK ZINC-BLENDE SEMICONDUCTORS

The only nonzero second-order nonlinear susceptibility tensor element for the $\bar{4}3m$ zinc-blende structure is the $\chi^{(2)}_{xyz}$ coefficient.[29] Existing calculations in the literature of the dispersion of the second-harmonic generation coefficient quote the form of Butcher and McLean[30] which includes the six terms for the transition scheme $a\rightarrow b\rightarrow c\rightarrow a$ (not including $a\rightarrow c\rightarrow b\rightarrow a$) where a corresponds to a valence band and b and c correspond to conduction bands.[37,38] It is not clear whether these calculations include correctly terms from the reverse transition order or from multiple valence bands. However, the dominant (half-band-gap) resonant term arises from the transition scheme $\Gamma^v_{15}\rightarrow\Gamma^c_1\rightarrow\Gamma^c_{15}\rightarrow\Gamma^v_{15}$ and since in GaAs and InSb the $\Gamma^c_{15}-\Gamma^c_1$ band gap is much larger than the fundamental $\Gamma^c_1-\Gamma^v_{15}$ band gap, the required correction for the partial cancellation (if necessary) is negligible.

In Fig. 2 the calculated dispersion of $\chi^{(2)}_{xyz}(\omega,\omega)$ using Eqs. (19) and (21) is shown for GaAs in the spectral region beneath the half band gap. The band structure model employed was a seven-band (Γ^v_{15}, Γ^c_1 and Γ^c_{15}) $\mathbf{k}\cdot\mathbf{p}$ model expanded around the Γ point.[39] Because this model does not provide an accurate representation of the band structure at the edge of the Brillouin zone there are two inconsistencies. First, an unphysical divergent term is introduced propor-

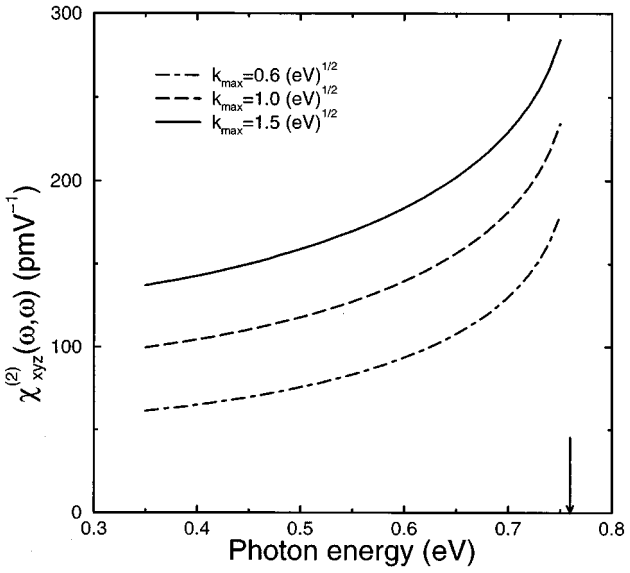

FIG. 2. Calculated dispersion of the second-order optical susceptibility $\chi^{(2)}_{xyz}(\omega,\omega)$ for GaAs using a seven-band model with a fundamental band gap of 1.519 eV. The three curves shown correspond to integrating over spheres of different radius in k space centered on the Γ point, $\sqrt{\hbar^2 k^2_{\max}/m_0}$=0.6, 1.0, and 1.5 (eV)$^{1/2}$. The arrow indicates the position of the half band gap $\hbar\omega = E_g/2$.

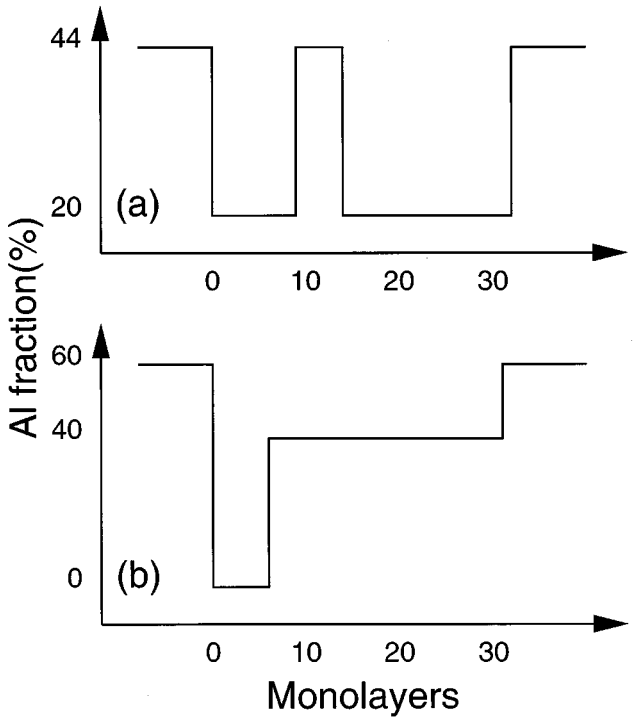

FIG. 3. Example asymmetric quantum well designs for second-harmonic generation using 1.55μm. (a) is a coupled quantum well with 9 and 18 monolayer thickness GaAs wells separated by a 5 monolayer thickness $Al_{0.4}Ga_{0.6}As$ barrier. (b) is a stepped quantum well consisting of a 6 monolayer thickness of GaAs and a 25 monolayer thickness of $Al_{0.4}Ga_{0.6}As$ surrounded by $Al_{0.6}Ga_{0.4}As$ barriers.

tional to ω^{-2}. The present calculation therefore expands the expression for the nonlinear susceptibility as a Laurent series and subtracts terms of this order. Second, the constant background contribution to the nonlinear susceptibility cannot be accurately obtained. This is apparent in Fig. 2 by noting the difference in result for integrating over the different volumes of k space shown. Note that the Brillouin zone corresponds roughly to $k_{\max} \simeq 1.5$ (eV)$^{1/2}$. The resonance feature, though, is determined by the states around the Γ point (direct gap) and is largely unaffected.

IV. ASYMMETRIC SEMICONDUCTOR HETEROSTRUCTURES

A [001]-grown asymmetric semiconductor heterostructure superimposes a $4mm$ tetragonal symmetry which induces second-order nonlinear coefficients $\chi^{(2)}_{xzx}$, $\chi^{(2)}_{zxx}$, and $\chi^{(2)}_{zzz}$.[29] There are two possible regimes for frequency conversion using such structures: long wavelength operation based solely on intersubband virtual transitions in doped structures ($\chi^{(2)}_{zzz}$ only) and near-ir operation based on a combination of interband and intersubband virtual transitions in intrinsic material.[12] For the long wavelength intersubband operation the effects of the partial cancellation will be limited as the $n=2$ to $n=3$ subband spacing is of a similar magnitude to the $n=1$ to $n=2$ subband spacing. However, in the case of the near-gap operation it is anticipated that the partial cancellation should have dramatic consequences as the upper level spacing (intersubband) is much smaller than the lower level spacing (interband). For example, in typical $GaAs/Al_xGa_{1-x}As$ quantum wells there is an order of magnitude difference between the intersubband separation and the band gap.

As examples, the asymmetric quantum well structures shown in Fig. 3 will be considered in this paper. These structures were initially designed such that the communications wavelength of 1.55 μm corresponds to a photon energy just beneath half of the band gap (such that any second harmonic generated lies in the transparency range of the material). The structures also contain a maximum of two different $Al_xGa_{1-x}As$ compositions in order to simplify the growth (only two aluminum sources will be required), but are otherwise similar to structures considered in earlier papers where second-order susceptibilities in the range $10-10^3$ pmV^{-1} are predicted.[15,16,20,22] In the expressions for the optical susceptibilities, both band energies and momentum matrix elements are required. The algorithm employed in this paper to determine these allows mixing of conduction band and heavy-hole, light-hole, and split-off valence band states and is described in the Appendix.

Figure 4 shows the valence band dispersion for the coupled quantum well example. Note that the asymmetry of this structure causes the Kramers spin degeneracy to be lifted. It is also apparent that the dispersion can only be approximated with a parabolic form over a very restricted region close to the Brillioun zone center and hence the envelope functions contain substantial mixtures of the basis Bloch functions. This has important repercussions for calculations of nonresonant optical constants (such as $\chi^{(2)}$) which require a summation over at least a significant fraction of the Brillioun zone.

An investigation of the envelope functions themselves also reveals a strong mixing of the basis Bloch functions. This will have a major influence on the optical matrix elements. As an example, for a typical $\sim$10 nm GaAs quantum

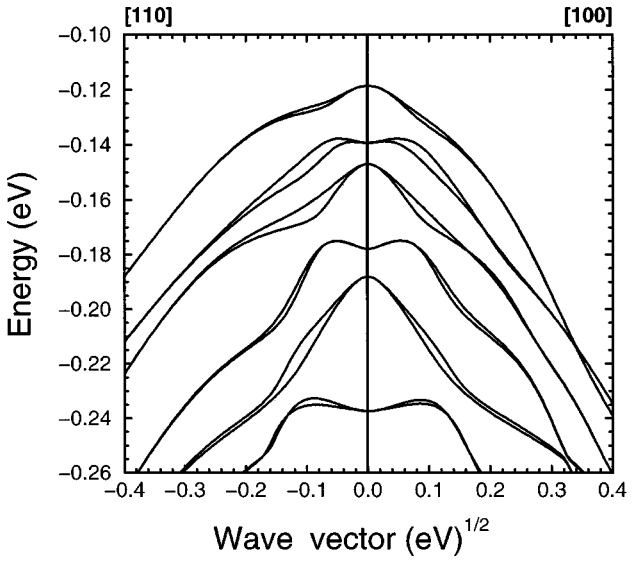

FIG. 4. Valence band dispersion for the asymmetric coupled quantum well used as an example here. The wave vector k has been scaled to $\sqrt{\hbar^2k^2/em_0}$ to give a value in $(\mathrm{eV})^{1/2}$. The asymmetry leads to a lifting of the Kramers degeneracy.

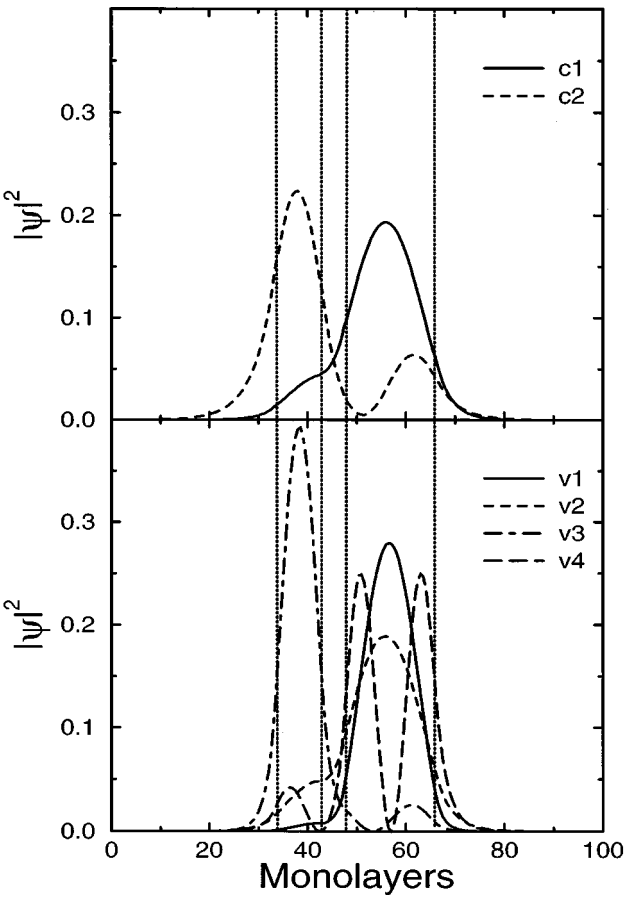

FIG. 5. Probability distribution $|\psi(z)|^2$ for the zone-center $(k_{\|}=0)$ conduction and valence band states for the asymmetric coupled quantum well. The states are labeled in order of energy with $v1$, $v3$, and $v4$ being predominantly heavy-hole states and $v2$ a light-hole state.

well, the lowest conduction bound state has $\sim$20% light-hole component to it. This is usually concealed within the effective mass approximation but for the detail of the matrix elements required here it is advisable to use a band structure model that allows full mixing of the basis Bloch functions. Showing all the components of an envelope function is unnecessarily complex to be plotted here but Figs. 5 and 6 show the probability distributions (sum of the moduli squared of the envelope function components) for two lowest conduction and five highest valence bound states. One consequence of this band mixing is that the probability distribution for the second bound conduction state does not have a minimum value of zero (even though the conduction envelope function component changes sign) due mainly to a finite light-hole component.

For the determination of the second-order susceptibilities Eqs. (19) and (21) are summed over sets of bound states (two conduction and five valence subbands) and integrated over k space [over the area of the circle defined by $k_{\|}\leqslant 0.6$ $(\mathrm{eV})^{1/2}$ which corresponds to roughly half the extent of the Brillioun zone]. The structures described in Fig. 3 are taken be repeated with a separation of 12 nm barriers in both cases. The quoted $\chi^{(2)}$ values are for the entire structure which should be borne in mind when comparing with other published values, some of which are quoted on a per-well basis. It is found that as the valence band dispersion is quite complex, the integrals generally have a slow convergence.

Figure 7 shows the dispersion of the three $\chi^{(2)}(\omega,\omega)$ [second-harmonic generation (SHG)] tensor elements as a function of detuning from the half band gap for the coupled quantum well example. Note that this band edge corresponds to the heavy-hole $n=1$ to conduction $n=1$ transition. For photon energies greater than the half band gap, the second harmonic generated will be absorbed and hence high conversion efficiencies are not possible. This can appear as an effective two-photon absorption of the fundamental.[40,41] It is clear from Fig. 7 that the tensor elements show a resonance at the half band gap, with the most resonant term being $\chi^{(2)}_{xzx}$. However, the valence band dispersion is intricate enough (i.e., nonparabolic) such that these resonances do not obey a simple power law and therefore do not appear as straight lines on a log-log plot. The reason that the xzx element is most resonant can be obtained by considering the momentum matrix elements between the heavy-hole $n=1$ and conduction $n=1,2$ subbands. Only the p_z matrix element is significant for the conduction intersubband transition and only the p_x (and p_y) matrix element is significant for heavy-hole/conduction interband transitions (as there is no z variation in the heavy-hole Bloch function). These combinations of matrix elements only appear in the most resonant terms in Eq. (19) $[(\Omega_{ab}-2\omega)$ as the denominator] for the xzx. Of course this is only a simplified description as there are other subbands to be summed over and the envelope functions do contain portions of other Bloch functions. The overall values are somewhat disappointing in that birefringent ferroelectrics used in practice for SHG have second-order susceptibilities of a few pmV^{-1} [no allowance has yet been made for the reduction in the conversion efficiency for quasi-phase-matching in comparison to full phase matching, e.g., by $(2/\pi)^2$ for domain reversal]. However, the predicted magnitude of the coefficients is comparable with recent experimental observations.[26–28]

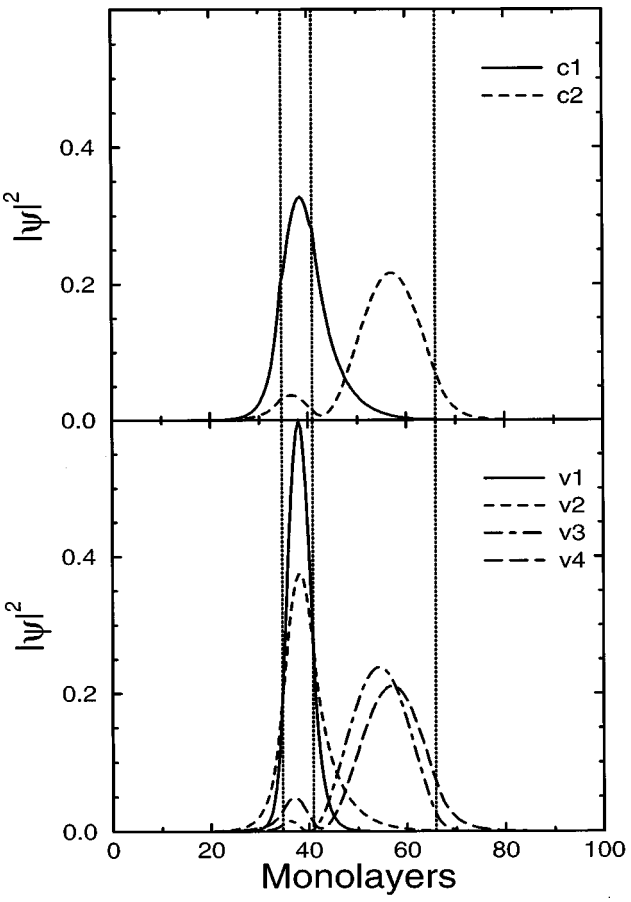

FIG. 6. Probability distribution $|\psi(z)|^2$ for the zone-center ($k_{\|}=0$) conduction and valence band states for the asymmetric stepped quantum well. The states are labeled in order of energy with $v1$ and $v3$ being predominantly heavy-hole states and $v2$ and $v4$, light-hole states.

Figure 8 shows the dispersion of the three $\chi^{(2)}(\omega,\omega)$ (SHG) tensor elements as a function of detuning from the half band gap for the stepped quantum well example. In contrast to the previous example, there is little indication of a resonance at the heavy-hole/conduction half band gap (also note the the xzx element is not the largest value). On examining the probability distributions in Fig. 6 it can be seen that there is almost no overlap between the $n=1$ heavy-hole state ($v1$) and the $n=2$ conduction band state. This is a result of the narrow, deep well (due to the growth restrictions) which ensures that the $n=1$ large effective mass states are highly confined. It seems reasonable to suggest that the optimal stepped well structure for resonant $\chi^{(2)}$ values will have similar layer widths and depths roughly in the ratio 1:2.

V. CONCLUSIONS

In this paper, the equivalents of the Maxwell-Bloch equations have been derived for a three-level system, specifically tailored for media with extended wave functions such as semiconductors. This formalism can be used to investigate several resonant nonlinear optical processes such as two-photon absorption, excited-state absorption, and electromagnetically induced transparency. Here nonresonant second-order processes are examined and complete expressions are

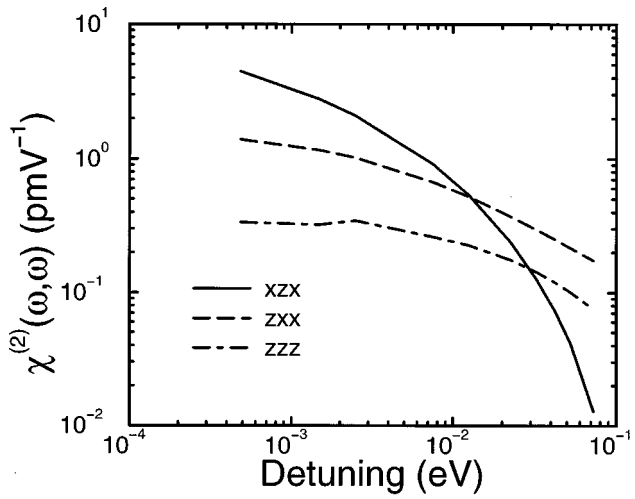

FIG. 7. Calculated dispersion of the $\chi^{(2)}$ tensor components for the asymmetric coupled quantum well example as a function of detuning from the half band gap (0.872 eV).

derived for the second-order optical susceptibility both for the case of single and double occupation. It is noted that a partial cancellation of terms occurs which can lead to a substantial overestimation of the nonlinear coefficient if only the most resonant term is retained. For the very large values of interband second-order susceptibility (>100 pmV^{-1}) predicted previously, only the equivalents of terms with denominators $(\Omega_{ab}-\omega_1-\omega_2)$ in Eq. (17) are retained (for example, Refs. 20 and 22). More reasonable values are obtained when the equivalent of terms with denominators $(\Omega_{ac}-\omega_1-\omega_2)$ are additionally included with the opposite sign. We note that the incorrect form of the second-order susceptibility with $\mathbf{E}\cdot\mathbf{r}$ and the incorrect substitution for the momentum matrix element in Refs. 15, 16, and 24 provides this partial cancellation and predicts a reasonable magnitude for the nonlinear coefficient. For quantum wells, this degree of cancellation is strongly influenced by the intersubband spacing.

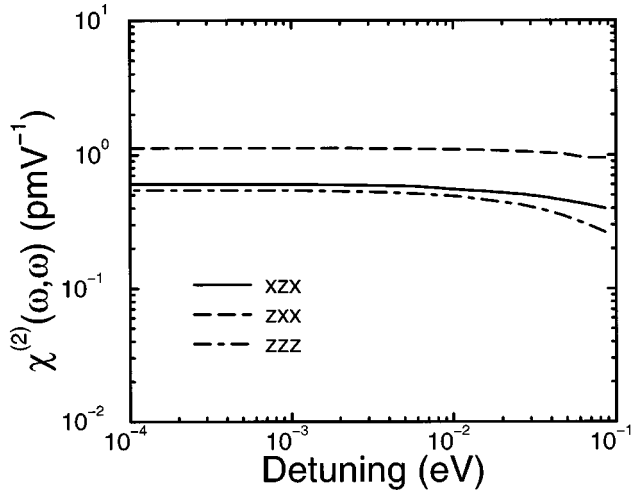

FIG. 8. Calculated dispersion of the $\chi^{(2)}$ tensor components for the asymmetric stepped quantum well example as a function of detuning from the half band gap (0.886 eV).

Two example $Al_xGa_{1-x}As$ asymmetric quantum well structures are analyzed for second-harmonic generation using a fundamental of wavelength around 1.5 μm. It is found that the only case of a coefficient which may be of some use was a few pmV^{-1} obtained near resonance for the xzx component in the coupled quantum well example. There is evidence that the nonparabolicity of the valence band dispersion has a major influence on the nonlinear coefficients. The stepped quantum well example demonstrates that it is not difficult to design a structure where the lack of overlap between the various bound states results in a small second-order nonlinearity. In the example calculations used in this paper only the contribution of the bound states have been included. The continuum states with energies greater than the barrier will also make a contribution but for photon energies below the half band gap this will be as a relatively small nonresonant background. For the cases where very small values are obtained it is likely that the relative contribution of the continuum states are significant but the overall magnitude of coefficient is still too small to be of any practical use.

Using the $\mathbf{A}\cdot\mathbf{p}$ form for the susceptibility allows some generalities to be made in discussing second-order nonlinear coefficients in semiconductors. Momentum matrix elements are basically a product of the Kane momentum parameter P (which has a similar value for all semiconductors) and an overlap integral. If the overlap integral is close to optimal, then the major influences on the magnitude of the coefficient are the frequency denominators and the number of electronic states. The expressions for the susceptibility in Eqs. (19) and (21) contain frequency denominators to the fifth power. Hence, providing it can be arranged to still operate at a resonance, long wavelength operation can have huge nonlinear coefficients. For example, increasing the wavelength by a factor of 10 will give five orders of magnitude increase in scaling of the nonlinear coefficient, which explains why huge coefficients are possible with (solely) intersubband transitions.[12] However, for a fixed wavelength of operation the major influence on the overall magnitude is the number of electronic states. For the unconfined dimensions the range of electronic wave vectors is $-\pi/a<k<\pi/a$ where a is the lattice constant. However, for a quantum well structure there is only one bound state per period L_p for each subband. Therefore with quantum confinement in one dimension the number of contributing states has been reduced in proportion to the factor a/L_p. In our examples, $a=0.565$ nm and $L_p\sim 20$ nm and therefore the upper limit that can be expected with structures of this size is around 1/40 of the bulk coefficient. This argument does not take account of all the details such as overlap integrals and precisely what interband momentum matrix elements contribute to the bulk result but does give an idea of the scaling involved.

This scaling argument also provides a clue into how larger second-order susceptibilities can be obtained with asymmetric growth: reduction of the quantum well structure period towards the lattice constant. Asymmetric short-period superlattices can potentially have nonlinear coefficients approaching the bulk value. Although conduction states in a superlattice are no longer localized this is not a problem since resonant carrier generation is avoided. Narrow, deep wells will also be of benefit in considering the partial cancellation of terms as the intersubband energy difference (or interminiband for superlattices) is increased. Asymmetric superlattices with layer thicknesses of one monolayer are not too dissimilar from the asymmetric structure in the [111] direction in a bulk zinc-blende structure which gives rise to a second-order susceptibility $\chi^{(2)}_{xyz}$ of around 300 pmV^{-1} in GaAs.[4] Similar types of structures arise with self-organized growth such as are observed in $Ga_{0.5}In_{0.5}P$.[42] Defining the asymmetry during growth allows quantum well disordering to be employed as a phase-matching technique. Potential asymmetric structures could consist of coupled wells (e.g., GaAs/AlAs/GaAs/AlAs superlattice with thicknesses in the ratio 1:1:2:2) or stepped wells (e.g., $GaAs/Al_{0.5}Ga_{0.5}As$/AlAs or GaAs/InAs/AlAs since thin layers can incorporate strain).

ACKNOWLEDGMENT

The Engineering and Physical Sciences Research Council is thanked for financial support.

APPENDIX: SEMICONDUCTOR HETEROSTRUCTURE BAND STRUCTURE

The band structure algorithm employed in the nonlinear optical coefficient calculations in this paper is a hybrid approach where explicit mixing of the lowest conduction band Γ_1^c and highest valence band set Γ_{15}^v occurs[43] but the semiempirical Luttinger-Kohn approach is used to account for interactions with other bands.[44] The exact envelope function form of Burt is used to derive the resulting 8×8 (asymmetric) interaction Hamiltonian matrix.[45,46] This can be subsequently block diagonalized with a suitable unitary transformation into two 4×4 *real* Hamiltonian matrices,[47]

$$H=\begin{bmatrix} E_c & \sqrt{3}T & T\pm\sqrt{2}iU & \sqrt{2}T\mp iU \\ \sqrt{3}T & -(E_1+E_2) & W\mp iS_{\|} & \sqrt{2}W\pm\dfrac{i}{\sqrt{2}}S_{\|} \\ T\mp\sqrt{2}iU & W\pm iS_{\|}^{\dagger} & -E_1+E_2\pm iC & -\sqrt{2}E_2\pm i\sqrt{\tfrac{3}{2}}\Sigma_{\|} \\ \sqrt{2}T\pm iU & \sqrt{2}W\mp\dfrac{i}{\sqrt{2}}S_{\|}^{\dagger} & -\sqrt{2}E_2\mp i\sqrt{\tfrac{3}{2}}\Sigma_{\|}^{\dagger} & -E_1-\Delta\mp iC \end{bmatrix}. \tag{A1}$$

The off-diagonal blocks contain only zero or small terms proportional to $\mu k_\parallel^2 \sin 4\phi$ which can be neglected. We define

$$E_c = E_{c0}(z) + \frac{s}{2}\,(k_\parallel^2 + k_z^2),$$

$$E_1 = -E_{v0}(z) + \frac{1}{2}\,(\gamma_1 k_\parallel^2 + k_z \gamma_1 k_z),$$

$$E_2 = -\xi(z) + \frac{1}{2}\,(\gamma_2 k_\parallel^2 - 2k_z \gamma_2 k_z),$$

$$T = \frac{1}{\sqrt{6}}\,P k_\parallel,$$

$$U = \frac{1}{2\sqrt{3}}\,(P k_z + k_z P),$$

$$W = -\frac{\sqrt{3}}{2}\,k_\parallel^2(\overline{\gamma} - \mu\,\cos 4\phi),$$

$$S_\parallel = \sqrt{3} k_\parallel \left[\left(\overline{\gamma} - \frac{3}{2}\,\delta\right) k_z + k_z \left(\mu + \frac{3}{2}\,\delta\right)\right],$$

$$C = k_\parallel [k_z(\overline{\gamma} \mu - 3\delta) - (\overline{\gamma} \mu - 3\delta) k_z],$$

$$\Sigma_\parallel = \frac{1}{\sqrt{3}}\,k_\parallel \left[\left(\overline{\gamma} + 2\mu + \frac{3}{2}\,\delta\right) k_z + k_z \left(2\overline{\gamma} + \mu - \frac{3}{2}\,\delta\right)\right],$$

$$\overline{\gamma} = \frac{1}{2}\,(\gamma_3 + \gamma_2),$$

$$\mu = \frac{1}{2}\,(\gamma_3 - \gamma_2),$$

$$\delta = \frac{1}{9}\,(1 + \gamma_1 + \gamma_2 - 3\gamma_3). \tag{A2}$$

Here E_{c0}, E_{v0}, and $(E_{v0} - \Delta)$ are the Γ-point energies (including hydrostatic strain), ξ is the shear-strain splitting energy, and P is the Kane momentum parameter.[43] The parameters s and the modified Luttinger-Kohn parameters γ_i represent the contribution to the effective mass from bands other than the set considered here (Γ_1^c and Γ_{15}^v). The in-plane electronic wave vector is given in terms of polar coordinates $(k_\parallel, \phi)$. The z-component of the electronic wave vector will be replaced by the differential operator $k_z \rightarrow -i\partial/\partial z$.

The method of solution is as follows. The heterostructure is discretized into N points in the z direction (typically $N \sim 200$) and the z derivatives are replaced with their corresponding finite differences. The $4N \times 4N$ matrix diagonalization is performed in real space, taking advantage of the sparseness of the matrix. This is performed in two stages: (1) the matrix is symmetrized to obtain all the eigenvalues then (2) selected eigenvalues (corresponding to bound solutions) are refined by inverse iteration using the correct asymmetric form of the Hamiltonian matrix, which also determines the eigenvectors. In calculating the optical constants, the energy eigenvalues and the momentum matrix elements (which can be obtained from overlap integrals of the eigenvectors) are required.

[1] F. Zernike and J. E. Midwinter, *Applied Nonlinear Optics* (Wiley, New York, 1973).

[2] Y. R. Shen, *The Principles of Nonlinear Optics* (Wiley, New York, 1984).

[3] G. I. Stegeman, D. J. Hagan, and L. Torner, Opt. Quantum Electron. **28**, 1691 (1996).

[4] M. M. Choy and R. L. Byer, Phys. Rev. B **14**, 1693 (1976).

[5] J. Khurgin, J. Appl. Phys. **64**, 5026 (1988).

[6] A. Fiore, V. Berger, E. Rosencher, N. Laurent, S. Theilmann, N. Vodjdani, and J. Nagle, Appl. Phys. Lett. **68**, 1320 (1996).

[7] M. J. Angell, R. M. Emerson, J. L. Hoyt, J. F. Gibbons, L. A. Eyres, M. L. Bortz, and M. M. Fejer, Appl. Phys. Lett. **64**, 3107 (1994).

[8] S. J. B. Yoo, R. Bhat, C. Caneau, and M. A. Koza, Appl. Phys. Lett. **66**, 3410 (1995); S. J. B. Yoo, C. Caneau, R. Bhat, M. A. Koza, A. Rajhel, and N. Antoniades, *ibid.* **68**, 2609 (1996).

[9] J. A. Armstrong, N. Bloembergen, J. Ducuing, and P. S. Pershan, Phys. Rev. **127**, 1918 (1962).

[10] A. Szilagyi, A. Hordik, and H. Schlossberg, J. Appl. Phys. **47**, 2025 (1976).

[11] M. K. Gurnick and T. A. DeTemple, IEEE J. Quantum Electron. **19**, 791 (1983).

[12] E. Rosencher, A. Fiore, B. Vinter, V. Berger, Ph. Bois, and J. Nagle, Science **271**, 168 (1996).

[13] D. C. Hutchings, C. Kelaidis, J. M. Arnold, J. S. Aitchison, C. N. Ironside, M. Street, and J. H. Marsh, *Nonlinear Optics: Materials, Fundamentals and Applications, Hawaii* (IEEE, Piscataway, NJ, 1994), p. 148.

[14] M. W. Street, N. D. Whitbread, C. J. Hamilton, B. Vögele, C. R. Stanley, D. C. Hutchings, J. H. Marsh, J. S. Aitchison, G. T. Kennedy, and W. Sibbett, Appl. Phys. Lett. **70**, 2804 (1997).

[15] J. Khurgin, Appl. Phys. Lett. **51**, 2100 (1987).

[16] J. Khurgin, Phys. Rev. B **38**, 4056 (1988).

[17] J. Khurgin, J. Opt. Soc. Am. B **6**, 1673 (1989).

[18] L. Tsang, D. Ahn, and S. L. Chuang, Appl. Phys. Lett. **52**, 697 (1988).

[19] L. Tsang, S. L. Chuang, and S. M. Lee, Phys. Rev. B **41**, 5942 (1990).

[20] P. J. Harshman and S. Wang, Appl. Phys. Lett. **60**, 1277 (1992).

[21] A. Shimizu, M. Kuwata-Gonokami, and H. Sakiki, Appl. Phys. Lett. **61**, 399 (1992).

[22] C. Kelaidis, D. C. Hutchings, and J. M. Arnold, IEEE J. Quantum Electron. **30**, 2998 (1994).

[23] R. Atanasov, F. Bassani, and V. M. Agranovich, Phys. Rev. B **50**, 7809 (1994).

[24] A. Fiore, E. Rosencher, B. Vinter, D. Weill, and V. Berger, Phys. Rev. B **51**, 13 192 (1995).

[25] Y. Huang, C. Wang, and C. Lien, IEEE J. Quantum Electron. **31**, 1717 (1995).

[26] S. Janz, F. Chatenoud, and R. Normandin, Opt. Lett. **19**, 622 (1994).

[27] X. H. Qu, H. Ruda, S. Janz, and A. J. SpringThorpe, Appl. Phys. Lett. **65**, 3176 (1994).
[28] A. Fiore, E. Rosencher, V. Berger, and J. Nagle, Appl. Phys. Lett. **67**, 3765 (1995).
[29] P. N. Butcher and D. Cotter, in *The Elements of Nonlinear Optics*, edited P. L. Knight and W. J. Firth, Cambridge Studies in Modern Optics Vol. 9 (Cambridge University Press, Cambridge, United Kingdom, 1990).
[30] P. N. Butcher and T. P. McLean, Proc. Phys. Soc. London **81**, 219 (1963).
[31] M. Gell-Mann and Y. Ne'eman, *The Eightfold Way* (Benjamin, New York, 1964).
[32] F. T. Hioe, Phys. Rev. A **28**, 879 (1983).
[33] P. K. Aravind, J. Opt. Soc. Am. B **3**, 1025 (1986).
[34] M. H. Weiler, Solid State Commun. **39**, 937 (1981).
[35] D. C. Hutchings and B. S. Wherrett, Phys. Rev. B **50**, 4622 (1994).
[36] B. S. Wherrett, Proc. R. Soc. London, Ser. A **390**, 373 (1983).
[37] M. I. Bell, in *Electronic Density of States*, edited by L. H. Bennett, Natl. Bur. Stand. (U.S.) Spec. Publ. 323 (U.S. GPO, Washington, DC, 1971), p.757.
[38] S. S. Jha and J. J. Wynne, Phys. Rev. B **5**, 4867 (1972).
[39] P. Pfeffer and W. Zawadzki, Phys. Rev. B **41**, 1561 (1990).
[40] J. S. Aitchison, D. C. Hutchings, J. U. Kang, G. I. Stegeman, and A. Villeneuve, IEEE J. Quantum Electron. **33**, 341 (1997).
[41] J. P. van der Ziel, Phys. Rev. B **16**, 2775 (1977).
[42] Y. Ueno, V. Ricci, and G. I. Stegeman, J. Opt. Soc. Am. B (to be published).
[43] E. O. Kane, J. Phys. Chem. Solids **1**, 249 (1957); in *Narrow Gap Semiconductors: Physics and Applications*, edited by W. Zawadzki, Lecture Notes in Physics Vol. 133 (Springer-Verlag, Berlin, 1980), p. 13.
[44] A. T. Meney, B. Gonul, and E. P. O'Reilly, Phys. Rev. B **50**, 10 893 (1994).
[45] M. G. Burt, J. Phys. Condens. Matter **4**, 6651 (1992).
[46] B. A. Foreman, Phys. Rev. B **48**, 4964 (1993).
[47] D. C. Hutchings and J. M. Arnold, *European Quantum Electronics Conference, Hamburg* (IEEE, Piscataway, NJ, 1996), p. 78.